Journal of Hazardous Materials 193 (2011) 156–163

Contents lists available at ScienceDirect

Journal of Hazardous Materials

journal homepage: www.elsevier.com/locate/jhazmat

Organically functionalized mesoporous SBA-15 as sorbents for removal of selected pharmaceuticals from water

Tung Xuan Bui [a], Seo-Young Kang [b], Sang-Hyup Lee [c], Heechul Choi [a,*]

[a] School of Environmental Science and Engineering, Gwangju Institute of Science and Technology (GIST), 261 Cheomdan-gwagiro, Buk-gu, Gwangju 500-712, Republic of Korea
[b] International Environmental Research Center (IERC), Gwangju Institute of Science and Technology (GIST), 261 Cheomdan-gwagiro, Buk-gu, Gwangju 500-712, Republic of Korea
[c] Water Environment Center, Korea Institute of Science and Technology, Cheongryang, Seoul 130-650, Republic of Korea

ARTICLE INFO

Article history:
Received 31 March 2011
Received in revised form 8 July 2011
Accepted 11 July 2011
Available online 20 July 2011

Keywords:
Adsorption
Pharmaceuticals
Functionalization
Mesoporous silica SBA-15
Trimethylsilyl groups

ABSTRACT

Mesoporous silica SBA-15 and its postfunctionalized counterparts with hydroxymethyl (HM-SBA-15), aminopropyl (AP-SBA-15), and trimethylsilyl (TMS-SBA-15) were prepared and characterized by powder X-ray diffraction, N_2 adsorption–desorption measurement, Fourier-transform infrared spectroscopy, and elemental analysis. The removal of a mixture of 12 selected pharmaceuticals was investigated by batch adsorption experiments onto SBA-15 and the grafted materials. SBA-15 showed to have moderate adsorption affinity with amino-containing (atenolol, trimethoprim) and hydrophobic pharmaceuticals, but it displayed minimal adsorption affinity toward hydrophilic compounds. HM-SBA-15 was analogous with SBA-15 in terms of the adsorption efficiency toward all pharmaceuticals. AP-SBA-15 exhibited an increase in the adsorption of two acidic compounds (clofibric acid, diclofenac) but a decrease in the adsorption of estrone and the two amino-containing compounds. Among the grafted materials, TMS-SBA-15 had the highest adsorption affinity toward most pharmaceuticals. Moreover, the adsorption of nine pharmaceuticals to TMS-SBA-15 was significantly higher than that to SBA-15; seven of which showed the removal percentages from 70.6% to 98.9% onto TMS-SBA-15. The number of pharmaceuticals showing high adsorption efficiency onto TMS-SBA-15 did not alter significantly as the pH changed in the range of 5.5–7.6. The results suggest that TMS-SBA-15 is a promising material for the removal of pharmaceuticals from aqueous phase, especially for the treatment of wastewater from drug manufacturers.

1. Introduction

Recently, pollution of pharmaceuticals in water is an environmental concern [1–3]. Numerous pharmaceuticals are ubiquitously detected in aqueous environment [2,4]. Unknown chronic ecotoxicities effects [4] together with antibiotic resistance issue [5] are making increasingly anxieties due to wide spreads of pharmaceuticals. The current technologies used in water treatment systems are not effective enough to eliminate many pharmaceuticals [6,7]. Therefore, treatment technologies that achieve effective pharmaceutical removal need to be developed. The treatment of wastewater from drug manufacturers and households, where pharmaceuticals are often present at $\mu g\,L^{-1}$ level [4,8] and even up to $100\,\mu g\,L^{-1}$ [9], should be considered with a priority.

Among several considered methods, adsorption has been receiving a lot of attention, due to its convenience once applied into current water treatment processes. Various types of sorbents have been proposed for the removal of pharmaceuticals, for example, activated carbon [10], zeolites [11], montmorillonite [12], and mesoporous silica [13]. Among them, mesoporous silica, first synthesized in 1992 [14], are good candidates for the adsorptive removal of pharmaceuticals since these materials have high surface area, large and uniform pore size, and tunable pore structure. Mesoporous silica SBA-15 was effective for the adsorption of neutral and acidic pharmaceuticals in acidic media [13], though its effectiveness was significantly reduced at a neutral pH because of its low point of zero charge. This shortcoming, fortunately, may be overcome by altering the surface chemistry of mesoporous silica by means of grafting with suitable functional groups. Recently, mesoporous silica SBA-15 was grafted with cobalt(II), nickel(II), and copper(II) amine complexes and then applied for the adsorption of naproxen [15]. Copper(II) amine supported SBA-15 showed high adsorption efficiency toward naproxen though alkaline conditions (pH 13) were needed.

Pharmaceutical compounds are known to have distinct physicochemical properties, particularly hydrophobicity ($\log K_{ow}$) and acidity (pK_a), which are often important characteristics of a sorbate in aqueous media. Pharmaceuticals are categorized from hydrophilic to hydrophobic and basic to acidic compounds [16]. A material used for the removal of pharmaceuticals, therefore,

* Corresponding author. Tel.: +82 62 715 2441; fax: +82 62 715 2434.
E-mail address: hcchoi@gist.ac.kr (H. Choi).

0304-3894/$ – see front matter © 2011 Elsevier B.V. All rights reserved.
doi:10.1016/j.jhazmat.2011.07.043

must have an adequate hydrophobicity and acidity, which can be achieved by grafting with a proper organic functional group on the surface. Organically functionalized mesoporous silica have demonstrated their potential in application for removal of various organic contaminants, such as aromatic compounds, dyes, and pesticides [17]. To the best of our knowledge, the use of mesoporous silica functionalized with different organic moieties for adsorption of pharmaceuticals in aqueous phase has yet to be reported elsewhere.

In the present study, SBA-15 was grafted with three different organic moieties such as aminopropyl, hydroxymethyl, and trimethylsilyl groups, which possess different hydrophobicity and acidity. SBA-15 and the grafted SBA-15 materials were then examined as sorbents for the adsorption of a mixture of pharmaceuticals in water. For this task, 12 pharmaceuticals were selected based on their frequent detection in aqueous environments [4,8], diverse properties in terms of hydrophobicity (K_{ow}) and acidity (pK_a), and different medication categories. A mixture of pharmaceuticals was used in all experiments, in accordance with real situations [2,18].

2. Experimental

2.1. Chemicals

Tetraethylorthosilicate (TEOS 98%, Aldrich), Pluronic P123 (BASF), hydrochloric acid (HCl, 37%, Sigma–Aldrich) (3-aminopropyl)triethoxysilane (APTES, 99%, Aldrich), hydroxymethyl triethoxysilane (HMTES, 50%, Gelest Inc.), hexamethyldisilazane (HMDS, 99%, Aldrich), anhydrous toluene (99.8%, Sigma–Aldrich), absolute ethanol (HPLC grade, Fisher scientific), and acetone (HPLC grade, Fisher scientific) were used for the synthesis and surface modification of SBA-15. Acetaminophen, atenolol, carbamazepine, clofibric acid, diclofenac sodium, estrone, gemfibrozil, ibuprofen, ketoprofen, sulfamethoxazole, and trimethoprim were purchased from Sigma–Aldrich; iopromide was obtained from United States Pharmacopeia. Nine surrogate standards include non-deuterated compounds (dihydrocarbamazepine, cloprop) obtained from Sigma–Aldrich and deuterated compounds (acetaminophen-d_4, atenolol-d_7, estrone-d_4, ibuprofen-d_3, iopromide-d_3, sulfamethoxazole-d_4, and trimethoprim-d_9) received from Toronto Research Chemicals. The purity of all chemicals used in this study is ≥97%. In addition, stock mixed solutions of all pharmaceuticals (100 mg L^{-1}) and surrogate standards (10 mg L^{-1}) were separately prepared in methanol and stored at −20 °C prior to use. The physicochemical properties of the studied compounds are presented in Table 1.

2.2. Preparation of sorbent materials

SBA-15 was synthesized using a method described elsewhere [13,19]. Monomeric organically functionalized SBA-15 materials were prepared using a post-grafting method. Firstly, calcined SBA-15 (1.0 g) was pretreated at 190 °C *in vacuo* for 6 h. The pretreated SBA-15 was then slurried in anhydrous toluene (100 mL) for 1 h under a dry N_2 flow. Next, an organosilane precursor (APTES, HMTES, and HMDS) in anhydrous toluene (50 mL) was added. An adequate amount of APTES (0.66 mL) and HMTES (1.26 mL) to make a monolayer of organic groups was used, whereas an excess amount of HMDS (5.90 mL) was employed. The reaction system was refluxed in the cases of alkoxysilanes (APTES, HMTES) but was kept at room temperature in the case of HMDS [20]; all reaction systems were stirred for 24 h under a dry N_2 flow. After reaction, the products were filtered and washed with toluene, ethanol, and acetone consecutively. Finally, the samples were dried *in vacuo* at 150 °C for 4 h and stored in a desiccator. The three functionalized

Table 1
Sorbate characteristics.

Compound	CAS No.	Use	MW	C_s (mg L^{-1})[a]	pK_a	δ[e]	$\alpha_{+/-}$ (%)[f]			$\log K_{ow}^{pHg}$		
							pH 5.5	pH 6.6	pH 7.6	pH 5.5	pH 6.6	pH 7.6
Acetaminophen	103-90-2	Analgesic	151.2	1.4×10^4	9.86[b], 9.38[c] [0/−][d]	−	0.0	0.1	0.6	0.48	0.47	0.47
Atenolol	29122-68-7	Beta blockers	266.3	1.33×10^4	9.43[b], 9.6[c] [+/0][d]	+	100.0	99.9	98.5	−3.70	−2.60	−1.60
Carbamazepine	298-46-4	Anti-epileptic	236.3	112	13.94[b] [0/−]	−	0.0	0.0	0.0	1.89	1.89	1.89
Clofibric acid	882-09-7	Lipid regulator	214.7	583	3.18[b] [0/−]	−	99.5	100.0	100.0	0.11	−0.99	−1.99
Diclofenac	15307-86-5	Arthritis	296.2	2.37	4.18[b], 4.15[c] [0/−]	−	95.4	99.6	100.0	3.20	2.12	1.12
Estrone	53-16-7	Steroid	270.4	30	10.25[b] [0/−]	−	0.0	0.0	0.2	3.62	3.62	3.62
Gemfibrozil	25812-30-0	Anti-chloresterol	250.3	10.9	4.75[b] [0/−]	−	84.9	98.6	99.9	3.49	2.45	1.46
Ibuprofen	15687-27-1	Pain reliever	206.3	21	4.41[b], 4.91[c] [0/−]	−	92.5	99.4	99.9	2.38	1.31	0.31
Iopromide	73334-07-3	X-ray contrast media	791.1	23.8	10.62[b] [0/−]; 12.36[b] [−/−−]	−	0.0	0.0	0.1	-2.66	−2.66	−2.66
Ketoprofen	22071-15-4	Pain reliever	254.3	51	4.23[b], 4.45[c] [0/−]	−	94.9	99.6	100.0	1.62	0.54	−0.46
Sulfamethoxazole	723-46-6	Antibiotic	253.3	610	1.39[b] [+/0], 5.81[b] [0/−]	−	32.9	86.1	98.4	0.57	0.078	−0.81
Trimethoprim	738-70-5	Antibiotic	290.3	400	7.04[b], 7.12[c] [+/0]	+	97.2	73.4	21.6	−0.97	0.012	0.49

[a] C_s denote water solubility; values come from SRC PhysProp (accessed on October 03, 2010).
[b] Values calculated with ACD/Labs pK_a dB v. 12 program.
[c] Values come from SRC PhysProp (accessed on October 03, 2010).
[d] [0/−], transitions from neutral to anionic form; [+/0], transitions from cationic to neutral form.
[e] The dominant ionized species at the tested pH range (5.5–7.6): anionic (−) and cationic (+).
[f] $\alpha_{+/-}$: Fraction of the dominant ionized species (%), calculated based on the pK_a values from ACD/Labs pK_a dB v. 12 program.
[g] K_{ow}^{pH}: pH-dependent octanol–water coefficient; values calculated with ACD/Labs LogD v. 12 program at zero ionic strength.

samples were named as AP-SBA-15 (aminopropyl groups), HM-SBA-15 (hydroxymethyl groups), and TMS-SBA-15 (trimethylsilyl groups).

2.3. Characterization

The synthesized materials were characterized by X-ray powder diffraction (XRD) using a PANalytical X'Pert PRO-MPD diffractometer with Cu Kα radiation (λ = 1.5406 Å) and operating at 40 kV and 25 mA. All XRD patterns were collected in the 2θ range of 0.5–10° with a scanning rate of 0.01°/s. Nitrogen adsorption–desorption measurements were carried out using a Micromeritics ASAP 2020 analyzer at −196 °C. Prior to each adsorption measurement, the SBA-15 and grafted samples were degassed at 200 °C for 6 h and 100 °C for 12 h, respectively. Fourier transform infrared (FTIR) spectra were recorded on a JASCO FTIR-460 Plus spectrometer via the KBr pellet method. The samples were analyzed at 8 cm^{-1} resolution and averaged over 300 scans in the absorption band range of 400–4000 cm^{-1}. CHN elemental analysis was conducted on an EA-1110 (Thermoquest) elemental analyzer. The percentage of carbon was utilized for calculating the surface coverage, α_{RP} (in μmol m^{-2}) with the following equation [21]:

$$\alpha_{RP} = \frac{10^6 P_C}{1200 n_C - P_C(M-1)} \frac{1}{S_{BET}} \quad (1)$$

where P_C (%) is the percentage of carbon determined via elemental analysis, n_C is the number of carbon atoms per silane moiety, M is the molar mass of the silane, and S_{BET} (m^2 g^{-1}) is the Brunauer–Emmett–Teller (BET) surface area of the unmodified silica. For trialkoxysilanes used in this study, the calculation of surface coverage values needs several assumptions: (i) all bonded silanes are attached to the surface via a single siloxane bridge and (ii) the residual ethoxy groups of the chemically bonded silanes were not hydrolyzed during the synthesis which occurred in a dry condition. The surface coverage of AP-SBA-15 material can also be estimated based on the percentage of nitrogen using a similar equation with the case of carbon.

2.4. Adsorption experiment

Batch adsorption experiments were studied in 40-mL amber vials containing 10 mg of the sorbents in 10 mL of aqueous solutions. The solution pH was controlled using either a 2 mM buffer of 2-(*N*-morpholino)ethanesulfonic acid (MES) (pH 5.5) or 3-(*N*-morpholino)propanesulfonic acid (MOPS) (pH 6.6 and 7.6), as needed. Preliminary experiments showed that MES and MOPS did not influence the adsorption of pharmaceuticals to SBA-15 and organically grafted SBA-15 materials. A sufficient volume of stock solution of pharmaceuticals were spiked to make an initial concentration of approximately 100 μg L^{-1} per compound and to ensure the fraction of methanol in the solution was <0.1%. In addition, sodium azide (100 mg L^{-1}) was added to inhibit aerobic biological activity during equilibration, and a total ionic strength of 10 mM was controlled by the addition of NaCl. Note that control samples containing no sorbents were prepared in parallel with every sample. The samples and controls were subsequently agitated in an incubator at 200 rpm at 25 °C for 24 h, which is sufficient for achieving adsorption equilibrium, as determined in preliminary experiments. Aliquots were then taken at the end of the 24 h period, filtered through a 0.2-μm cellulose acetate membrane filter (Advantec MFS) before being extracted by solid-phase extraction (SPE) and analyzed using an LC–tandem MS. All experiments were replicated three or four times.

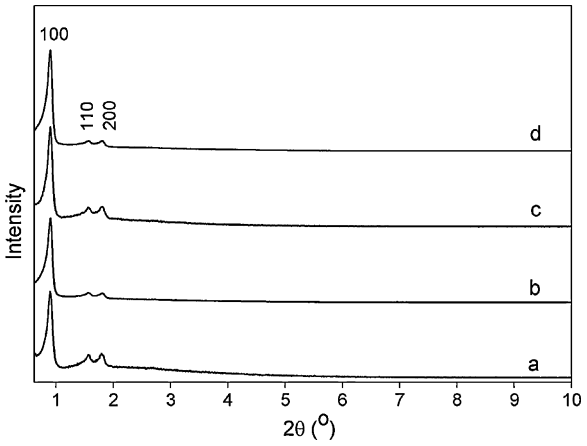

Fig. 1. X-ray diffraction patterns of (a) SBA-15, (b) HM-SBA-15, (c) AP-SBA-15, and (d) TMS-SBA-15.

2.5. Sample preparation and analytical methods

Prior to analysis, the filtrate was spiked with a surrogate standard solution to make a concentration of 50 μg L^{-1} per compound and extracted through 3 mL, 60 mg Oasis HLB cartridges (Waters). Pharmaceuticals were analyzed on an LC–tandem MS system equipped with a Waters Alliance 2695 HPLC system, a Waters Micromass Quattro micro API mass spectrometer, and a Waters Sunfire C_{18} column (150 mm × 2.1 mm i.d., 3.5 μm, 100 Å, end-capped C_{18} particles). The methods used for SPE and LC–tandem MS were adapted from literature [13,22] with a few modifications. Sample preparation and analysis are described in detail in Section S1 of the Supporting Information (SI).

2.6. Data analysis

The adsorption percentage of each pharmaceuticals was calculated based on the difference between the concentration (C_i, μg L^{-1}) in the control and the concentration (C_f, μg L^{-1}) in the samples after adsorption. To evaluate the adsorption capability of a sorbent, surface-area normalized adsorption coefficient (K_d, mL m^{-2}) of each pharmaceuticals toward the sorbent was calculated using the following equation:

$$K_d = \frac{C_i - C_f}{C_f} \frac{V_{sol}}{m_{ads}} \frac{1}{S_{BET}} \quad (2)$$

where V_{sol} (mL) is the volume of the solution, m_{ads} (g) is the mass of the sorbent used, and S_{BET} (m^2 g^{-1}) is the BET surface area of the sorbent material.

3. Results and discussion

3.1. Characterization of the synthesized materials

The XRD patterns of SBA-15 samples before and after modification (Fig. 1) all displayed an intense diffraction peak at about 2θ of 0.9°, which is characteristic of a mesostructure. Moreover, two additional peaks were observed in the XRD patterns, which can be indexed as (1 1 0) and (2 0 0) reflections of a hexagonal *P6mm* symmetry [19]. The results demonstrate that the periodic ordered structure of SBA-15 was maintained after modification. However, spacing values (a_o) of the grafted SBA-15 samples reduced somewhat (see Table 2), compared to SBA-15, indicating changes in their wall thickness and pore size due to the deposition of organosilane.

The nitrogen adsorption isotherms of SBA-15 and three grafted SBA-15 materials had similar patterns as a type IV isotherm and

Table 2
Structural properties of the sorbent materials.

Sample	a_o (nm)	S_{BET} ($m^2\ g^{-1}$)	V_{total} ($cm^3\ g^{-1}$)	D_{pore} (nm)	t_{wall} (nm)	% Carbon	% Nitrogen	Surface coverage ($\mu mol\ m^{-2}$)
SBA-15	11.4	837	1.04	7.2	4.2	0.12	nd	
HM-SBA-15	11.2	686	0.85	6.8	4.4	3.81	nd	0.81
AP-SBA-15	11.2	461	0.65	6.4	4.8	7.27	1.33	1.36[a]
TMS-SBA-15	11.2	565	0.75	6.7	4.5	5.29	nd	1.91

a_o: XRD unit-cell parameter calculated as $a_o = 4 \times d(200)/\sqrt{3}$; V_{total}: total pore volume; D_{pore}: primary mesopore size; t_{wall}: silica wall thickness, calculated as $a_o - D_{pore}$. nd: not detectable.

[a] The value was calculated based on the nitrogen percentage.

a hysteresis loop type H1 (Fig. 2); hysteresis loops with sharp adsorption and desorption branches are indicative of a narrow pore size distribution. Fig. 2 also shows that the nitrogen adsorbed amount decreases as SBA-15 is grafted with organic groups. The structural parameters calculated from nitrogen adsorption measurements are presented in Table 2. In the table, it is shown that the specific surface area, pore volume, and pore size of the samples followed the order: SBA-15 > HM-SBA-15 > TMS-SBA-15 > AP-SBA-15, whereas the inverse order was observed in terms of wall thickness. The significant decreases in the surface area of the grafted samples in comparison with SBA-15 confirm the attaching of organic groups inside the pores.

The CHN elemental analysis data (Table 2) also provide an evidence for the presence of the organic groups in the grafted materials. Moreover, the data were used for the calculation of the surface coverage of these groups. For AP-SBA-15, the surface coverages calculated from the carbon (1.20 $\mu mol\ m^{-2}$) and nitrogen percentage (1.36 $\mu mol\ m^{-2}$) agree within 10% for each phase. The surface coverage of the grafted groups followed the sequence: HM-SBA-15 (0.81 $\mu mol\ m^{-2}$) < AP-SBA-15 (1.36 $\mu mol\ m^{-2}$) < TMS-SBA-15 (1.91 $\mu mol\ m^{-2}$). It should be noted that the surface coverages of the grafted groups are lower than a full coverage of the SBA-15 of 4–6 $\mu mol\ m^2$ [23]. This characteristic implies that a high amount of residual surface silanol groups remains in the grafted samples, which would follow the reverse order of the surface coverage: HM-SBA-15 > AP-SBA-15 > TMS-SBA-15.

The presence of the attached organic groups in the modified samples can be further confirmed using FTIR, as shown in Fig. 3. The spectra of all the materials contain the typical Si–O–Si bands around 1080–1200 and 458 cm^{-1} associated with the formation of a condensed silica network and a broad band centered at 3420 cm^{-1} and a strong peak around 1630 cm^{-1} assigned to O–H bonds in silanol groups and adsorbed water molecules [24]. These bands (3420 and 1630 cm^{-1}) indicate that the grafted samples contain residual silanol groups and adsorbed water molecules. A weak peak associated with non-condensed Si–OH groups around 965 cm^{-1} [24] was found in the spectra of SBA-15 and HM-SBA-15 but it became unresolved in AP-SBA-15 and discernable in TMS-SBA-15. The results demonstrate that the amount of Si–OH groups was utilized most in TMS-SBA-15, followed by AP-SBA-15 and HM-SBA-15, which is consistent with the surface coverage of these materials (see Table 2). Bands at 1300–1470 and 2800–3000 cm^{-1} associated with aliphatic CH vibration were found in HM-SBA-15, AP-SBA-15, and especially in TMS-SBA-15. Weak absorption bands in the region of 1300–1470 cm^{-1} assigned to CH_3 asymmetrical bending (1470 cm^{-1}), CH_3 symmetrical bending (1380 cm^{-1}), CH_2 scissoring (1465 cm^{-1}), and CH_2 wagging modes (1305 cm^{-1}) can be observed in the spectra of the three grafted samples. In the region of 2800–3000 cm^{-1}, the peaks found in the spectrum of HM-SBA-15 (2983, 2934, and 2904 cm^{-1}), AP-SBA-15 (2935, 2904, and 2875 cm^{-1}), and TMS-SBA-15 (2964, 2906, and 2858 cm^{-1}) can be assigned to the stretching vibration of methyl and methylene groups. The presence of a weak band at 691 (N–H bending), 1510 (the symmetry $-NH_2$ bending), and 1558 cm^{-1} (the NH_2 deformation mode [24,25]) confirms the incorporation of amino groups in AP-SBA-15. Meanwhile, a sharp absorption band at 849 cm^{-1} and two small shoulder peaks at 816 and 760 cm^{-1} were found in the spectrum of TMS-SBA-15, which are assigned to Si–C stretching vibrations and CH_3 rocking [26].

3.2. Adsorption of pharmaceuticals

Adsorption experiments of a mixture of 12 pharmaceuticals were investigated onto grafted SBA-15 materials and were compared to bare SBA-15 to evaluate the adsorption efficiencies of the materials and figure out the role of surface functional groups and physico-chemical properties of pharmaceuticals in the adsorption. The adsorption affinity of sorbents was judged using the surface-

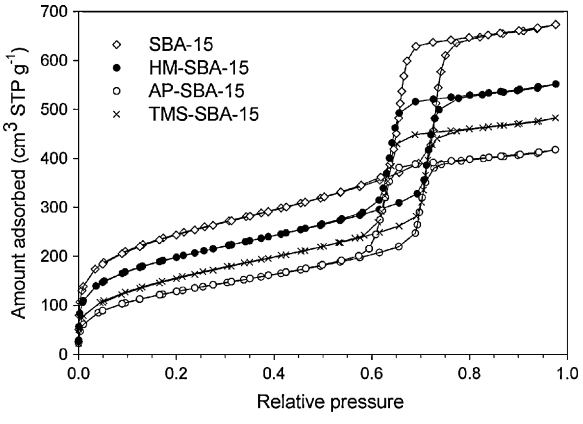

Fig. 2. Nitrogen adsorption isotherms for SBA-15, HM-SBA-15, AP-SBA-15, and TMS-SBA-15 samples.

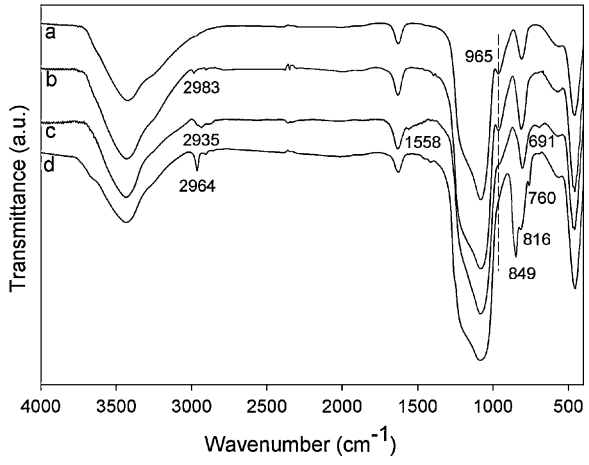

Fig. 3. FTIR spectra of (a) SBA-15, (b) HM-SBA-15, (c) AP-SBA-15, and (d) TMS-SBA-15.

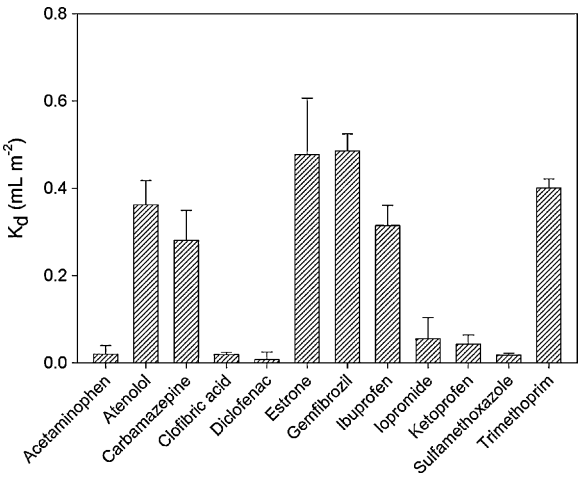

Fig. 4. The adsorption coefficient (K_d) of pharmaceuticals toward SBA-15 at pH 5.5. Error bars represent the standard deviation of sample replicates.

area normalized adsorption coefficient (K_d) calculated by Eq. (2) to eliminate the difference in the surface area among the sorbents.

3.2.1. Adsorption of pharmaceuticals to SBA-15

Since the point of zero charge of SBA-15 was estimated at 4.0 [13], the SBA-15 surface is negatively charged at the studied pH conditions. Hence, it was expected that the electrical charge of pharmaceuticals plays an important role in their adsorption onto SBA-15. Twelve pharmaceuticals can be classified into three groups based on their dominant species at the studied pH (see Table 1): cationic (atenolol and trimethoprim), neutral (acetaminophen, carbamazepine, estrone, and iopromide), and anionic compounds (clofibric acid, diclofenac, gemfibrozil, ibuprofen, ketoprofen, and sulfamethoxazole).

The adsorption of pharmaceuticals to SBA-15 at pH 5.5 is presented in Fig. 4. Six compounds showed remarkable adsorption ($K_d > 0.1\ mL\ m^{-2}$) to SBA-15, which included two cationic (atenolol, trimethoprim), two neutral (carbamazepine, estrone), and two anionic compounds (gemfibrozil, ibuprofen). Nevertheless, the adsorption percentages of the compounds were all below 30% (Fig. S1, SI). The other six compounds including two neutral (acetaminophen, iopromide) and four anionic compounds (clofibric acid, diclofenac, ketoprofen, sulfamethoxazole) did not reveal significant adsorption to SBA-15 (Fig. 4). It was found that in the same group of properties (i.e., neutral, cationic, and anionic) the compounds having a higher hydrophobicity (K_{ow}^{pH}) (see Table 1) generally produced higher adsorption capacities, except for diclofenac. This result suggests that hydrophobic interaction may play an important role in the adsorption of the pharmaceuticals onto SBA-15 [27]. On the other hand, the adsorption of two cationic compounds was comparable to that of the neutral and anionic compounds, despite the lower hydrophobicity (K_{ow}^{pH}) of the cationic compounds (Table 1). This point demonstrates that the electrostatic attraction between cationic compounds and negatively charged sites on the surface of SBA-15 is of great importance in the adsorption of these compounds.

3.2.2. Adsorption of pharmaceuticals to HM-SBA-15

The adsorption coefficients of pharmaceuticals toward HM-SBA-15 were observed to be comparable to those toward SBA-15 (Fig. 5a). In addition, the *t*-test results suggest that there were not statistically significant differences ($p > 0.05$) between the adsorption coefficients of all pharmaceuticals to HM-SBA-15 and SBA-15. A possible explanation for the results is that the difference in hydrophobicity and acidity between HM-SBA-15 and SBA-15 might be not large enough to cause significant changes in their adsorption toward pharmaceuticals. Although hydroxymethyl groups in HM-SBA-15 are more hydrophobic and less acidic than silanol groups, the low fraction of hydroxymethyl groups ($0.81\ \mu mol\ m^{-2}$) compared to the residual surface silanol groups ($3–5\ \mu mol\ m^{-2}$) might be the main reason for the similarities in the adsorption of pharmaceuticals onto HM-SBA-15 and SBA-15.

3.2.3. Adsorption of pharmaceuticals to AP-SBA-15

The adsorption of pharmaceuticals onto AP-SBA-15 and SBA-15 at pH 5.5 is exhibited in Fig. 5b. It was expected that AP-SBA-15 may have preferable adsorption to acidic pharmaceuticals [28,29] owing to acid–base and/or electrostatic interaction formed between amino groups in AP-SBA-15 and carboxylic groups in acidic pharmaceuticals. This expectation found true in the cases of clofibric acid and diclofenac; the K_d values of clofibric acid and diclofenac toward AP-SBA-15 were significantly higher ($p < 0.05$) than those toward SBA-15 (Fig. 5b). In contrast, the K_d values of atenolol, estrone, and trimethoprim toward AP-SBA-15 were significantly lower ($p < 0.05$) than those toward SBA-15. The adsorption of the seven remaining compounds onto AP-SBA-15 was not statistically significantly different ($p > 0.05$) from that onto SBA-15.

Theoretically, the presence of amino groups in AP-SBA-15 may cause both advantages and drawbacks to the adsorption of pharmaceuticals. The presence of hydrophilic amino groups on the surface of AP-SBA-15 possibly impairs the adsorption of hydrophobic compounds; this might be the case for the lower adsorption of extremely hydrophobic estrone ($\log K_{ow} = 3.62$, Table 1) to AP-SBA-15 in comparison with SBA-15. On the other hand, existing as cationic ($–NH_3^+$) or neutral ($–NH_2$) form on the surface at pH

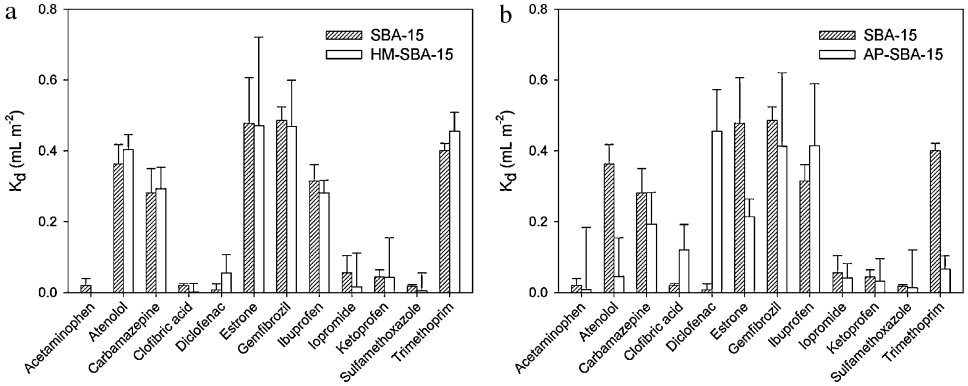

Fig. 5. The adsorption coefficient (K_d) of pharmaceuticals toward (a) HM-SBA-15 and (b) AP-SBA-15 in comparison with SBA-15 at pH 5.5. Error bars represent the standard deviation of sample replicates.

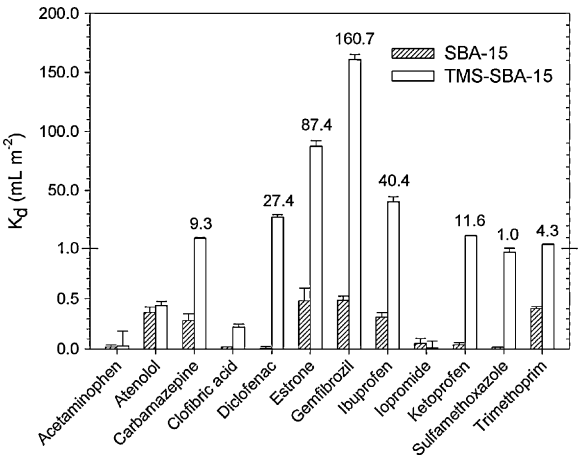

Fig. 6. The adsorption coefficient (K_d) of pharmaceuticals toward TMS-SBA-15 in comparison with SBA-15 at pH 5.5. Error bars represent the standard deviation of sample replicates.

5.5, amino groups result an increase in the surface charge [28], thereby inducing the adsorption of anionic species of anionic compounds via electrostatic interaction. Meanwhile, the adsorption of neutral species of these acidic compounds may be favorably implemented onto $-NH_2$ sites through acid–base interaction. A higher surface charge of AP-SBA-15, however, would result a decrease in the adsorption of cationic compounds due to a higher electrostatic repulsion. The amino groups may also interact with weakly acidic surface silanol groups (≡SiOH, ≡SiO$^-$) via hydrogen bonding or electrostatic interaction [30], which then block the surface silanol groups; this may be beneficial for the approach of anionic compounds to the surface, whereas it may harm the adsorption of cationic compounds. These hypotheses apparently support the fact that AP-SBA-15 had higher adsorption affinity toward two anionic compounds (clofibric acid, diclofenac) but lower adsorption affinity toward two cationic compounds (atenolol, trimethoprim) than SBA-15. It is not well understood why the adsorption of the other acidic pharmaceuticals onto AP-SBA-15 was not improved significantly. In all probability, a balance of the positive and negative factors results in the comparable adsorption of the seven pharmaceuticals to AP-SBA-15 and SBA-15.

3.2.4. Adsorption of pharmaceuticals to TMS-SBA-15

Whereas HM-SBA-15 and AP-SBA-15 showed unmarked changes in the adsorption of pharmaceuticals in comparison with SBA-15, TMS-SBA-15 displayed intensive increases ($p < 0.05$) in the adsorption of nine pharmaceuticals, except for acetaminophen, atenolol, and iopromide, as shown in Fig. 6. The K_d values of the nine compounds toward TMS-SBA-15 were ten (clofibric acid, trimethoprim) to thousand times (diclofenac) higher than those to SBA-15. In particular, seven compounds, including carbamazepine (K_d = 9.3 mL m^{-2}), diclofenac (K_d = 27.4), estrone (K_d = 87.4), gemfibrozil (K_d = 160.7), ibuprofen (K_d = 40.4), ketoprofen (K_d = 11.6), and trimethoprim (K_d = 4.3), had extremely high adsorption affinity to TMS-SBA-15. The adsorption percentages of the seven compounds were as high as 70.6–98.9% (Fig. S2, SI).

The high adsorption efficiency of pharmaceuticals onto TMS-SBA-15 can be attributed to the fact that TMS-SBA-15 has a higher hydrophobicity [31] and a lower negative surface charge density [32], compared to SBA-15. The replacement of surface silanol groups in SBA-15 by hydrophobic trimethylsilyl (TMS) groups allows to increase the hydrophobicity of the material but also reduces the number of surface silanol groups. Obviously, a more hydrophobic and less charged TMS-SBA-15 will be more attractive to both hydrophobic and anionic compounds. In general, pharmaceuticals with a higher hydrophobicity in the same groups showed a higher K_d value (Fig. 6), for example, gemfibrozil > ibuprofen > diclofenac > ketoprofen > sulfamethoxazole > clofibric acid, estrone > carbamazepine, and trimethoprim > atenolol (see Table 1). The predominance of hydrophobic interaction between pharmaceuticals and TMS-SBA-15 is also supported by the fact that the adsorption affinity of TMS-SBA-15 was low toward hydrophilic compounds, such as acetaminophen, atenolol, and iopromide.

3.2.5. Influence of pH to the adsorption of pharmaceuticals

Since pH is always an important factor in adsorption processes, the adsorption of pharmaceuticals onto TMS-SBA-15 was performed at a range of naturally occurring pH values (5.5–7.6). In parallel, the adsorption of pharmaceuticals as a function of pH was examined in the case of SBA-15 for comparison. The adsorption percentages of pharmaceuticals onto SBA-15 and TMS-SBA-15 at different pH are shown in Fig. 7. As the pH increased from 5.5 to 7.6, the pH-dependent adsorption behavior of many pharmaceuticals was almost similar for TMS-SBA-15 and SBA-15. There were three distinct relationships observed between pharmaceutical adsorption onto TMS-SBA-15 and pH (Fig. 7b); interestingly, each relationship corresponded to a group of compounds having similar pK_a values and the same predominant species. The figure shows that the pH did not result in any statistically significant change ($p > 0.05$) in the adsorption of neutral compounds to TMS-SBA-15. However, the adsorption of carbamazepine and estrone onto SBA-15 decreased ($p < 0.05$) as the pH increased from

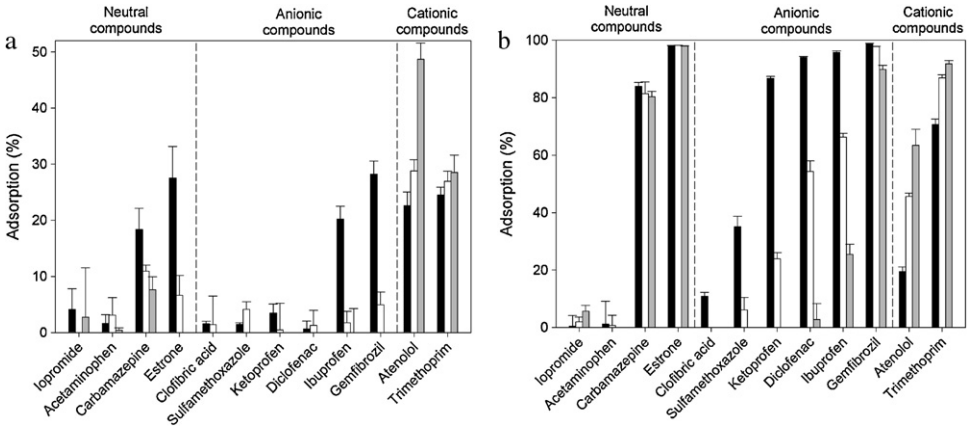

Fig. 7. The adsorption percentages (%) of pharmaceuticals onto (a) SBA-15 and (b) TMS-SBA-15 at different solution pHs: 5.5 (■), 6.6 (□), and 7.6 (▩). Error bars represent the standard deviation of sample replicates.

5.5 to 6.6 (Fig. 7a). Fig. 7b also shows that as the pH increased the adsorption of cationic compounds onto TMS-SBA-15 gradually increased, whereas the adsorption of anionic compounds to the material sharply decreased. The analogous results were observed for the adsorption of these compounds onto SBA-15, except for trimethoprim (Fig. 7a). The adsorption of trimethoprim onto SBA-15 did not show significant changes ($p > 0.05$) as the pH increased, though an increasing trend of the average values was detected. As a whole, the adsorption of pharmaceuticals onto TMS-SBA-15 was highly efficient at different pH values; the pharmaceuticals showing adsorption percentages of >80% included six compounds at pH 5.5 and four compounds at pH 6.6 and 7.6 (Fig. 7b).

In the same group of compounds (i.e. neutral, cationic, and anionic), the adsorption percentages of pharmaceuticals onto TMS-SBA-15 were observed to follow a solid order, regardless of the solution pH: (i) estrone > carbamazepine > acetaminophen ≈ iopromide for neutral compounds; (ii) gemfibrozil > ibuprofen > diclofenac > ketoprofen > sulfamethoxazole > clofibric acid for anionic compounds; and (iii) trimethoprim > atenolol for cationic compounds (Fig. 7b). Apparently, the order of adsorption percentages among the compounds in one group is consistent with their pH-dependent octanol–water coefficient (K_{ow}^{pH}) (see Table 1), except for the case of diclofenac. These results indicate that hydrophobic interaction is of great importance in the adsorption of pharmaceuticals to TMS-SBA-15. Note that the lower adsorption affinity of diclofenac in comparison with ibuprofen was observed at all pH values not only for TMS-SBA-15 but also for SBA-15 (see Fig. 7a) in this study and in a previous report [13]. However, the reasons behind these phenomena are not yet well understood.

The similar pH-dependent adsorption behavior of anionic and cationic pharmaceuticals onto SBA-15 and TMS-SBA-15 can be attributed to the similarity in some of their structural characteristics; the surface of the two materials is dominant by silanol groups. In addition, TMS groups on the surface of TMS-SBA-15 are not changed by the solution pH. Therefore, the changes of pharmaceutical adsorption are essentially responsible by alteration of surface silanol groups and pharmaceutical properties under different pH conditions. Silanol groups (≡Si–OH) are known as hydrophilic and ionizable groups, which are then ionized and turned into negatively charged groups (≡SiO^-) as the pH increases, resulting a higher negative-charge density on the surfaces of materials. Meanwhile, as the pH increases, anionic compounds are ionized and changed from neutral species into anionic species—a more hydrophilic one (see Table 1). The adsorption of these anionic species would be disfavored on SBA-15 and TMS-SBA-15 surfaces with a higher number of negatively charged sites (≡SiO^-) due to electrostatic repulsion, thereby leading a reduction in the adsorption of anionic compounds as the pH increases. In contrast, as the pH increases, cationic compounds are turned from cationic species to neutral species—a more hydrophobic one (Table 1). For TMS-SBA-15, the adsorption of neutral species of cationic compounds to TMS groups is more preferred than their corresponding cationic species, whereas the cationic species can be favorably adsorbed on negative charge sites (≡SiO^-) via electrostatic attraction. Consequently, as the pH increased the adsorption of cationic compounds onto TMS-SBA-15 increased. The unique difference in the adsorption of cationic compounds onto SBA-15 in comparison with that onto TMS-SBA-15 is without the enrollment of TMS groups.

Because neutral compounds are uncharged and unchanged as the pH increases, the adsorption of these compounds onto SBA-15 and TMS-SBA-15 is solely influenced by a higher ionization of surface silanol groups. The ionization of surface silanols results in a decrease in the hydrophobicity of sorbents. The constant adsorption capacity of neutral compounds to TMS-SBA-15 as the pH varies, therefore, can be attributed to a minimal reduction in hydrophobicity of TMS-SBA-15, which, in turn, is possibly due to its high hydrophobicity. In contrast, an increase in ionization of silanol groups on the surface of SBA-15 may reduce its hydrophobicity a significant amount. As a result, the adsorption of carbamazepine and estrone onto SBA-15 decreased significantly as the pH increased.

4. Conclusions

In the study, the adsorption of a mixture of pharmaceuticals to SBA-15 and three grafted SBA-15 was investigated and compared with each other. SBA-15 had moderate adsorption affinity with amino-containing (atenolol, trimethoprim) and hydrophobic compounds, but for hydrophilic ones, no significant adsorption was observed. The adsorption of all pharmaceuticals onto HM-SBA-15 was comparable to that onto SBA-15. Similar results were also observed for the adsorption of seven compounds onto AP-SBA-15, except that an increase in the adsorption of two acidic compounds (clofibric acid and diclofenac) and a decrease in the adsorption of estrone and two cationic compounds onto AP-SBA-15 were obtained in comparison with SBA-15. In comparison with SBA-15 and the other grafted SBA-15 materials, TMS-SBA-15 had the highest adsorption capacities toward most pharmaceuticals; seven compounds showed the adsorption percentages > 70% onto TMS-SBA-15 at pH 5.5. In addition, the change of the solution pH in the range of 5.5–7.6 may alter the adsorption efficiency of individual pharmaceuticals onto TMS-SBA-15 but the whole efficiency of all pharmaceuticals was not significantly varied. The results in the study suggest that TMS-SBA-15 may be applicable for the removal of pharmaceuticals from aqueous phase, especially for the treatment of wastewater from drug manufacturers. Further investigations are in progress to find out the effect of chemical factors to the adsorption of pharmaceuticals onto TMS-SBA-15 as well as the regeneration of the sorbent.

Acknowledgement

This research was supported by Korea Ministry of Environment as Converging Technology project.

Appendix A. Supplementary data

Supplementary data associated with this article can be found, in the online version, at doi:10.1016/j.jhazmat.2011.07.043.

References

[1] S.K. Khetan, T.J. Collins, Human pharmaceuticals in the aquatic environment: a challenge to green chemistry, Chem. Rev. 107 (2007) 2319–2364.
[2] D.W. Kolpin, E.T. Furlong, M.T. Meyer, E.M. Thurman, S.D. Zaugg, L.B. Barber, H.T. Buxton, Pharmaceuticals, hormones, and other organic wastewater contaminants in U.S. streams, 1999–2000: a national reconnaissance, Environ. Sci. Technol. 36 (2002) 1202–1211.
[3] M.J. Benotti, R.A. Trenholm, B.J. Vanderford, J.C. Holady, B.D. Stanford, S.A. Snyder, Pharmaceuticals and endocrine disrupting compounds in U.S. drinking water, Environ. Sci. Technol. 43 (2009) 597–603.
[4] K. Fent, A.A. Weston, D. Caminada, Ecotoxicology of human pharmaceuticals, Aquat. Toxicol. 76 (2006) 122–159.
[5] J.L. Martinez, Antibiotics and antibiotic resistance genes in natural environments, Science 321 (2008) 365–367.
[6] P.E. Stackelberg, E.T. Furlong, M.T. Meyer, S.D. Zaugg, A.K. Henderson, D.B. Reissman, Persistence of pharmaceutical compounds and other organic wastewater contaminants in a conventional drinking-water-treatment plant, Sci. Total Environ. 329 (2004) 99.
[7] S. Castiglioni, R. Bagnati, R. Fanelli, F. Pomati, D. Calamari, E. Zuccato, Removal of pharmaceuticals in sewage treatment plants in Italy, Environ. Sci. Technol. 40 (2006) 357–363.
[8] A. Pal, K.Y.-H. Gin, A.Y.-C. Lin, M. Reinhard, Impacts of emerging organic contaminants on freshwater resources: review of recent occurrences, sources, fate and effects, Sci. Total Environ. 408 (2010) 6062–6069.

[9] D.G.J. Larsson, C. de Pedro, N. Paxeus, Effluent from drug manufactures contains extremely high levels of pharmaceuticals, J. Hazard. Mater. 148 (2007) 751–755.
[10] Z. Yu, S. Peldszus, P.M. Huck, Adsorption characteristics of selected pharmaceuticals and an endocrine disrupting compound—Naproxen, carbamazepine and nonylphenol—on activated carbon, Water Res. 42 (2008) 2873–2882.
[11] A. Rossner, S.A. Snyder, D.R.U. Knappe, Removal of emerging contaminants of concern by alternative adsorbents, Water Res. 43 (2009) 3787–3796.
[12] Z.B. Molu, K. Yurdakoç, Preparation and characterization of aluminum pillared K10 and KSF for adsorption of trimethoprim, Microporous Mesoporous Mater. 127 (2010) 50–60.
[13] T.X. Bui, H. Choi, Adsorptive removal of selected pharmaceuticals by mesoporous silica SBA-15, J. Hazard. Mater. 168 (2009) 602–608.
[14] C.T. Kresge, M.E. Leonowicz, W.J. Roth, J.C. Vartuli, J.S. Beck, Ordered mesoporous molecular sieves synthesized by a liquid-crystal template mechanism, Nature 359 (1992) 710–712.
[15] S.M. Rivera-Jiménez, S. Méndez-González, A. Hernández-Maldonado, Metal ($M = Co^{2+}$, Ni^{2+}, and Cu^{2+}) grafted mesoporous SBA-15: effect of transition metal incorporation and pH conditions on the adsorption of Naproxen from water, Microporous Mesoporous Mater. 132 (2010) 470–479.
[16] E.H. Kerns, L. Di, Drug-Like Properties: Concepts, Structure Design and Methods: from ADME to Toxicity Optimization, Academic Press, 2008.
[17] A. Walcarius, L. Mercier, Mesoporous organosilica adsorbents: nanoengineered materials for removal of organic and inorganic pollutants, J. Mater. Chem. 20 (2010) 4478–4511.
[18] K. Kümmerer, The presence of pharmaceuticals in the environment due to human use—present knowledge and future challenges, J. Environ. Manage. 90 (2009) 2354–2366.
[19] D. Zhao, J. Feng, Q. Huo, N. Melosh, G.H. Fredrickson, B.F. Chmelka, G.D. Stucky, Triblock copolymer syntheses of mesoporous silica with periodic 50–300 angstrom pores, Science 279 (1998) 548–552.
[20] R. Anwander, I. Nagl, M. Widenmeyer, G. Engelhardt, O. Groeger, C. Palm, T. Röser, Surface characterization and functionalization of MCM-41 silicas via silazane silylation, J. Phys. Chem. B 104 (2000) 3532–3544.
[21] G.E. Berendsen, L. de Galan, Preparation and chromatographic properties of some chemically bonded phases for reversed-phase liquid chromatography, J. Liq. Chromatogr. 1 (1978) 561–586.
[22] B.J. Vanderford, S.A. Snyder, Analysis of pharmaceuticals in water by isotope dilution liquid chromatography/tandem mass spectrometry, Environ. Sci. Technol. 40 (2006) 7312–7320.
[23] I.G. Shenderovich, G. Buntkowsky, A. Schreiber, E. Gedat, S. Sharif, J. Albrecht, N.S. Golubev, G.H. Findenegg, H.-H. Limbach, Pyridine-^{15}N A mobile NMR sensor for surface acidity and surface defects of mesoporous silica, J. Phys. Chem. B 107 (2003) 11924–11939.
[24] X. Wang, K.S.K. Lin, J.C.C. Chan, S. Cheng, Direct synthesis and catalytic applications of ordered large pore aminopropyl-functionalized SBA-15 mesoporous materials, J. Phys. Chem. B 109 (2005) 1763–1769.
[25] C.-H. Chiang, H. Ishida, J.L. Koenig, The structure of γ-aminopropyltriethoxysilane on glass surfaces, J. Colloid Interface Sci. 74 (1980) 396–404.
[26] A.J. Van Roosmalen, J.C. Mol, An infrared study of the silica gel surface. 1. Dry silica gel, J. Phys. Chem. 82 (1978) 2748–2751.
[27] O. Lorphensri, J. Intravijit, D.A. Sabatini, T.C.G. Kibbey, K. Osathaphan, C. Saiwan, Sorption of acetaminophen, 17 α- ethynyl estradiol, nalidixic acid, and norfloxacin to silica, alumina, and a hydrophobic medium, Water Res. 40 (2006) 1481–1491.
[28] D. Zhu, H. Zhang, Q. Tao, Z. Xu, S. Zheng, Surface functionalized mesoporous silicas as adsorbents for aromatic contaminants in aqueous solution, Environ. Toxicol. Chem. 28 (2009) 1400–1408.
[29] M. Anbia, M. Lashgari, Synthesis of amino-modified ordered mesoporous silica as a new nano sorbent for the removal of chlorophenols from aqueous media, Chem. Eng. J. 150 (2009) 555–560.
[30] M.W. McKittrick, C.W. Jones, Toward single-site functional materials preparation of amine-functionalized surfaces exhibiting site-isolated behavior, Chem. Mater. 15 (2003) 1132–1139.
[31] T. Takei, A. Yamazaki, T. Watanabe, M. Chikazawa, Water adsorption properties on porous silica glass surface modified by trimethylsilyl groups, J. Colloid Interface Sci. 188 (1997) 409–414.
[32] V.M. Gun'ko, O.E. Voronina, E.F. Voronin, V.I. Zarko, E.M. Pakhlov, R. Leboda, J. Skubiszewska-Zieba, W. Janusz, S. Chibowski, Nanosilica partially modified by hexamethyldisilazane in air, Polish J. Chem. 79 (2005) 1787–1804.